Cumhuriyet Sci. J., 43(2) (2022) 327-332
DOI: https://doi.org/10.17776/csj.1085276

Cumhuriyet Science Journal

| csj.cumhuriyet.edu.tr | Founded: 2002 ISSN: 2587-2680 e-ISSN: 2587-246X Publisher: Sivas Cumhuriyet University

Variation of Pinning Force Density Throughout the TSMG Y123 Superconductor with Location

Bakiye Çakır [1,a,*]

[1] *Vocational School of Health Services, Artvin Çoruh University, Artvin, Türkiye.*
**Corresponding author*

Research Article

History
Received: 09/03/2022
Accepted: 05/05/2022

ABSTRACT

Top seeded melt growth (TSMG) Y123 sample with 35 mm diameter was produced by using Nd123 seed and its superconducting parameters such as transition temperature (T_c), critical current density (J_c) and pinning mechanism were locally examined by taking small specimens which are containing defects in different number, size and distribution from different locations throughout the sample. The T_c of the main sample was determined from the resistivity measurement as 93.4 K. It was observed that the J_c was higher in the region close to the seed, while the J_c decreased towards to the edge or the deeper regions of the sample. Effective pinning mechanisms at different temperatures were determined by plotting the curves of the pinning force density (f_p) of the specimens versus reduced magnetic field ($h = H_a/H_{max}$) and the locational variations of the f_p were examined. It was seen that below the value of $h \approx 0.2$, normal point pinning was dominant at 30 and 50 K, while surface pinning was dominant at 77 K, in the all specimens. In addition, a transition was observed between two different pinning mechanisms when the $H_{max} > h > 0.2$. The transition was took place between $\Delta\kappa$ and normal point pinning at 30 and 50 K while it was seen between $\Delta\kappa$ and surface pinning at 77 K.
.

Keywords: Pinning force density, Critical current density, Local variation of superconductivity, TSMG Y123.

[a] *bcakir@artvin.edu.tr* *https://orcid.org/0000-0003-4339-1913*

Introduction

Discovery of the high temperature superconductor (HTS) which offer a superconducting transition at the liquid nitrogen temperature have been lead to many studies on the usability of superconductors in both materials science and its engineering applications. It is essential to achieve high superconducting properties such as critical current density (J_c), critical transition temperature (T_c) and field trapping capabilities for the applications [1-3]. On the other hand the magnetic field penetrates in the form of vortices in the HTSs and vortices can move easily when the temperature approaches the T_c or when high fields are applied. At that case, the J_c value is suppressed by thermal fluctuations and the increasing applied magnetic field due to the vortex motion caused by the effect of the Lorentz force [4]. Therefore, the vortices are needed to pin into the crystals to improve the J_c by introducing effective pinning centers in the form of impurities and defects (such as oxygen vacancies, dislocations, aggregation defects, chemical additives and secondary phase particles) [5]. Additionally, the sizes of these defects must be in the nanometer range [6].

The HTSs are generally produced by annealing the samples, which are pressed in the selected composition with appropriate methods and heat treatments. The Y123 single crystals grow basically in a structure with non-superconducting green inclusions called the Y211 phase entrapped and distributed throughout the matrix. The obtained superconducting samples can be single or multi grained. For this reason it is important to determine the optimum conditions for the fabrication of the sample in order to obtain a high current carrying capacity. It is possible to produce large single-grained samples aligned in the *c*-axis direction with the melting methods and especially top seed melt growth (TSMG) and infiltration growth (IG) methods are promising. Generally, seeds having a higher melting temperature and a similar crystal structure to the main sample are used in these methods [7-12].

On the other hand, since J_c in two-phase alloys is affected by the size and distribution of the second phase particles, the selected region cut from the sample affects the J_c value. Even J_c values can be change throughout the sample. If the small sections selected from multi-grain samples include in grain boundaries, micro cracks or different size and distribution of the pinning centers, it would be also effect the J_c value. So the superconducting properties of the melt growth bulk superconductor generally change with the position in the volume [13, 14]. In this study, the J_c values of the specimens taken from different parts of the TSMG Y123 sample were calculated and the regional variations of the pinning force densities and pinning mechanism were examined at different temperatures

Material and Method

The powder mixture prepared in Y_2O_3: $BaCO_3$: CuO = 1:2:3 stoichiometric ratio was calcined in an alumina

crucible at 900°C for 30 hours with an intermediate grinding. The powder mixture was ground again after the calcination process and completely melted at 1450°C in a platinum crucible. The melted powder mixture poured onto a copper plate and cooled quickly by hitting with another copper plate. Thin plates obtained after the melting process was ground again and Y123 starting powder was prepared. 40 g of the starting powder was weighed and pressed into a 35 mm diameter pellet under 11 tons/cm^2 pressure. The Nd123 seed was placed in top surface center of the sample pressed into the pellet and the sample was placed on an alumina substrate with Y_2O_3 powder. The sample was growth by applying the heat treatment given in Figure 1. After all, the grown Y123 sample was annealed for 200 hours at 500°C in oxygen atmosphere.

Resistivity and magnetization measurements were made by taking small specimens from the Y123 sample obtained after crystal growth process. The location of the specimens (a, b, c and d) is schematically given in the Figure 2 and they were labeled as Y-a, Y-b, Y-c and Y-d. Y-a, Y-b and Y-c were used for magnetization measurements and Y-d was used resistivity measurement

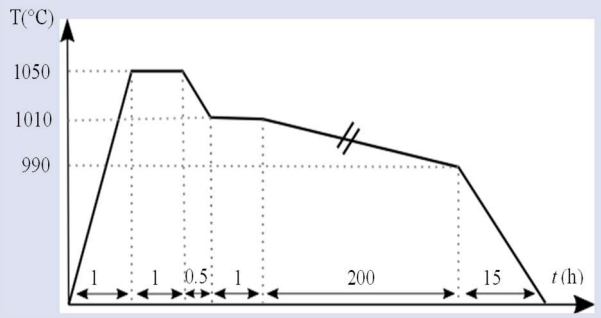

Figure 1. Thermal process of the crystal growth for TSMG Y123.

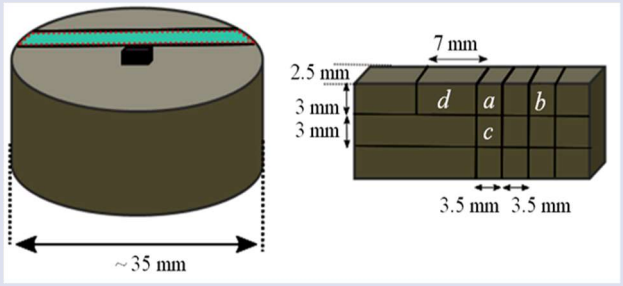

Figure 2. Schematic drawing of the specimen locations cut from the TSMG Y123 sample.

Apparatus

X-ray diffraction data were collected from the sample and small specimens cut from the main sample after the upper surfaces of the sample were cleaned by sanding and polished by using a Rikagu D/Max III C diffractometer, employing CuKα (λ = 1.5418 Å, 40 kV, 30 mA) radiation

Standard four probe resistivity measurement of the Y-d sample was performed at temperatures between 60 and 100 K at 0 T magnetic field using a PPMS. The magnetization measurements were operated by using VSM module of the PPMS system at constant temperatures 30, 50 and 77 K at a sweep speed of 100 Oe/s and by applying a magnetic field parallel to the *c*-axis between −5T and +5T. All the measurements were performed in zero-field cooling (ZFC) regime.

The critical current densities J_c (A/cm^2) of the specimens have been estimated from the magnetization measurements by using the extended Bean model as given the below equation.

$$J_c = 20\Delta M/a(1 - a/3b) \quad (1)$$

where ΔM is the width of the magnetization curve in emu·cm^{-3}, a and b ($a < b$) are the dimensions of the rectangular cross section of the sample in cm.

Pinning mechanism was determined by using Dew-Hughes model [15]. The Dew-Hughes model of elementary pinning forces ($F_p = J_c \times B$) is generally expressed with normalized pinning force density, $f_p = F_p/F_{p,max}$ and often scales with reduced field $h = (H_a/H_{irr})$ is the ratio between applied magnetic field external H_a and irreversibility field H_{irr} (where $F_p = 0$) which can be determined from magnetoresistivity, AC susceptibility and magnetization measurements. The scaling of $f_p - h$ for the HTS is often analyzed using the Equations (2-4) [16, 17].

$$f_p(b) = 3b^2(1 - 2b/3) \quad \Delta\kappa \text{ pinning} \quad (2)$$

$$f_p(b) = (9b/4)(1 - b/3)^2 \quad \text{Normal point pinning} \quad (3)$$

$$f_p(b) = (25\sqrt{b}/16)(1 - b/5)^2 \quad \text{Surface pinning} \quad (4)$$

Dislocations or needle-shaped precipitation are the point pinning centers and they can interact with only one flux line. Twin planes, grain boundaries and plane-like precipitation are the surface pinning centers. The large precipitation and thick-walls dislocations from cell-structures are the Δκ pinning (volume pinning) centers [18].

Results and Discussion

.

Synthesis and Characterization

X-ray diffraction patterns of the main Y123 sample and small specimens cut from the different position of the Y123 sample are shown in Figure 3. Main sample Y123 and the Y-a, Y-b and Y-c specimens have predominantly (00ℓ) orientation peaks and small amount of the non-superconducting Y211 inter phase formed by the heat treatment process was also observed in the structure. This indicates that the sample has almost single-crystal

structure and a preferential orientation in the c-axis direction. The preferred orientations of HTS result to higher Jc [19]. In addition, the presence of the he Y211 phases are known to function as pinning centers in Y123 samples produced by melting process. On the other hand, the specimens Y-b located near the corner and Y-c located near the bottom of the sample have also extra low intensity peak of Y211 phase different from the Y-a. This situation states that non superconducting residual phases increase with increasing distance from the seed.

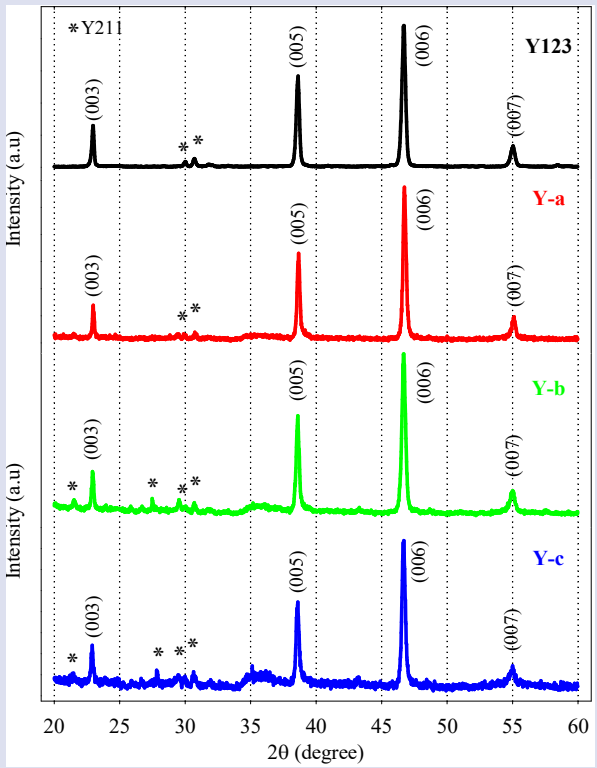

Figure 3. X-ray diffraction pattern of TSMG Y123 sample and Y-a, Y-b and Y-c specimens cut from the sample.

Electrical Investigation

The resistivity-temperature curve of the Y-d specimen during heating at 0T magnetic field and the temperature change curve of *dR/dT* determined the T_c transition temperature at which the superconducting state starts are given in Figure 4. Transition temperature T_c was determined as 93.4 K from the maximum peak position of the *dR/dT* curve and the transition gap (ΔT_c) obtained full width half maximum of the curve was approximately 1 K. Shortness of the transition is due to the single grain property or strong inter-granular connection.

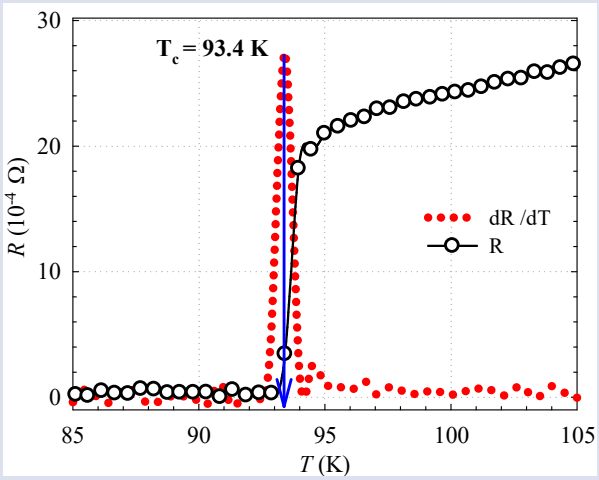

Figure 4. The resistivity-temperature curve of the Y-d specimen under 0 T magnetic field and the *dR/dT* curve determined the T_c value.

Magnetic Investigation

Figure 5 shows the variation of J_c calculated from the Bean critical state model against the external magnetic field for Y-a, Y-b and Y-c specimens at 30, 50 and 77 K. In the low magnetic field and high temperature region, J_c decreases quickly with the temperature. It is clearly seen in Figure 5 that J_c changes slightly with the increasing field at 30 and 50 K. This variation shows that all specimens are resistant to the external magnetic field and this case observed in single crystal superconductors. In addition, there is no explicit difference between all the specimens, there are only small variations. The specimen Y-a cut from the near the seed at first layer had clearly higher J_c rather than the Y-b cut from far the seed at first layer and Y-c cut from the second layer. It is well known that the J_c, decrease as the distance the seed location on the upper surface center of the sample increases [14]. The J_c decreases much more when the operated temperature approaches the T_c because of the flux pinning created by the linear correlated disorders such as interfaces between the Y211 particles and Y123 grains [20]. Even so, it is seen that the J_c value in 77 K does not decrease to zero even under 4T area. The high J_c value in 77 K shows the quality of the sample and it's preferred for technological applications. Homogeneity of the different phases and particles into the main matrix can be change with the position for the melt growth bulk superconductors and so the superconducting properties can be changed. It was thought that one of the reasons for this is that the distribution and the size of the 211 particles that acting as the pinning center in the structure. Because the applied magnetic field starts to penetrate into the structure at constant temperatures with the increasing field, the superconductivity weakens and J_c decreases due to mobility of the vortex [21]. The other reason is that the composition of the melt varies continuously during the melt process. The local microstructure and the local properties are defined from the melt composition [13].

.

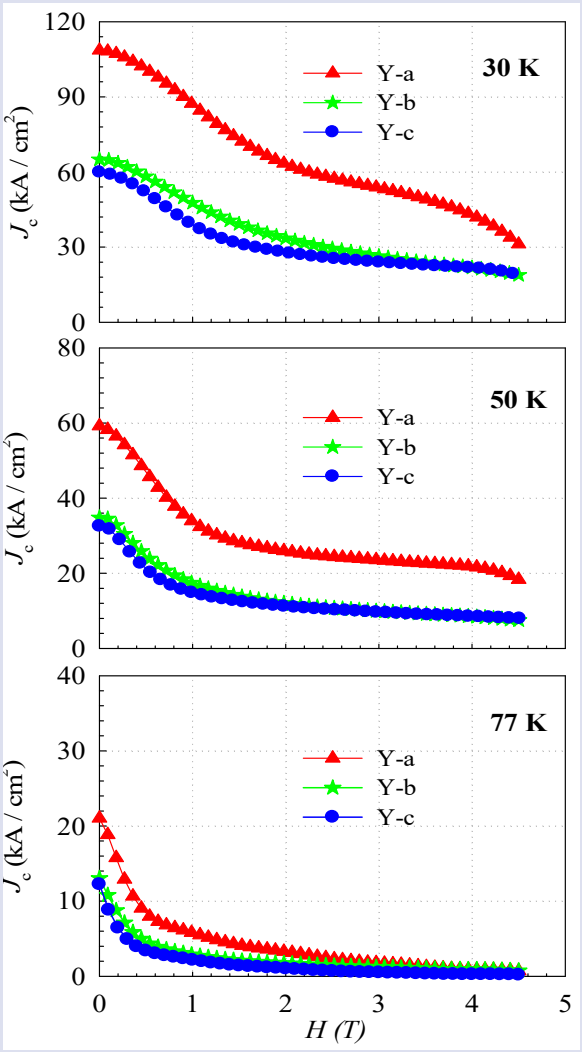

Figure 5. Critical current densities at 30, 50 and 77 K in the ZFC regime as a function of applied magnetic field for Y-a, Y-b and Y-c specimens.

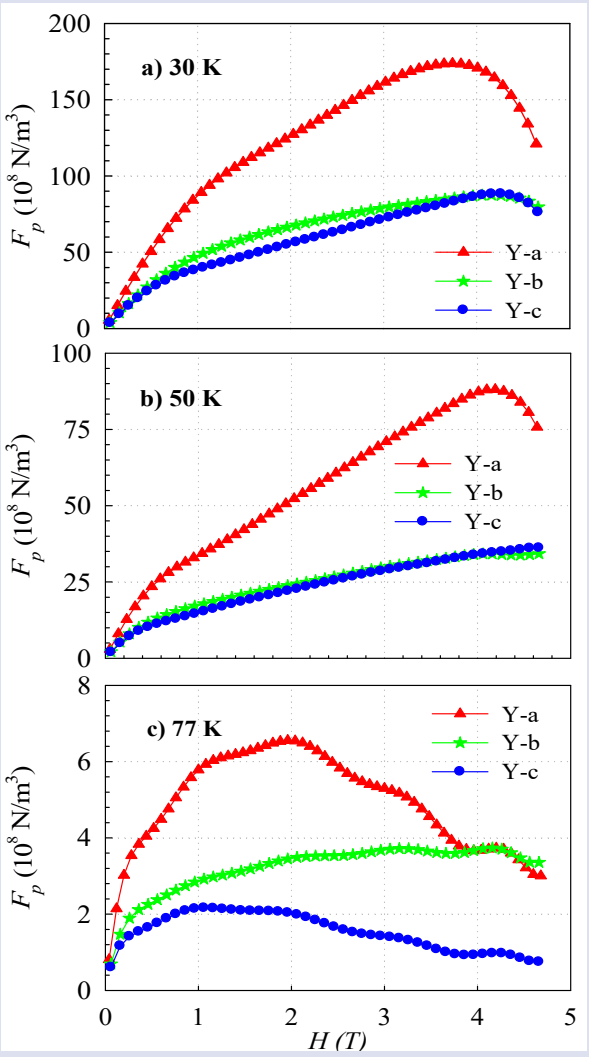

Figure 6. Plots of the volume pinning force (F_p) as a function of applied magnetic field for the Y-a, Y-b and Y-c samples at a) 30 K, b) 50 K and c) 77 K.

In order to study the nature of the pinning mechanism, firstly the volume pinning force were calculated. The volume pinning forces, F_p, scaled in a function of the applied magnetic field for all the specimens at 30, 50 and 77 K and were given in Figure 6. In contrast to the J_c, F_p always gives a maximum peak at H_{max}, before the F_p reaching zero at the irreversibility field (H_{irr}). Since the F_p value does not drop to zero in the applied field, it is difficult to determine the H_{irr} value precisely for HTS. Therefore, H_{max} value was used instead of H_{irr} [17]. H_{max} values were determined as 3.74, 4.15 and 4.22 T at 30 K, 4.16, 4.68 and 4.63 T at 50 K and 1.97, 4.16 and 1.08 T at 77 K for the Y-a, Y-b and Y-c, respectively. $F_p(H)$ curves exhibit growing curvatures at low fields and low temperatures and the curve began to fall down after the peak value at high fields as 30 K and 50 K. On the other hand, the shape of the curvatures distorted at 77 K as the transition temperature is approached. Also, Y-a had a much greater pinning force than Y-b and Y-c as expected from the J_c results.

The normalized volume pinning force density $f_p = F_p/F_{p,max}$ (where $F_{p,max}$ is the maximum pinning force) are plotted versus the reduced magnetic field $h = H_a/H_{max}$ in Figure 7. Equations (2)-(4) are also presented in the Figure 7. Dotted line represents that $\Delta\kappa$ pinning, the dashed line represents normal ($\Delta\ell$) point pinning and the solid line represents surface pinning. It is well known that HTSs have large κ values and core pinning is dominant rather than magnetic interaction in the superconductors. The core pinning leaves two different sources called δl and $\Delta\kappa$ (or δT_c) pinning [22]. δl pinning centers are very effective at low fields and low temperatures and the centers behave like normal conducting particles embedded in the superconducting matrix. On the other hand, $\Delta\kappa$ pinning centers are effective at the intermediate areas and temperatures, as they act as local oxygen deficient regions [23]. As shown in Figure 7, the specimens scaled in agreement below $h \approx 0.2$ (low field region) with Equation (3), stating that the samples are predominantly affected by the normal point pinning at 30 and 50 K. The major defects in this category are the dislocation and needle

shape Y211 precipitations. When the magnetic fields increase a value between the $h \approx 0.2$ and H_{max}, intermediate field region, the results are not scaled on a single theoretical curve. That is the plots are located between Δκ and normal point pinning. Because Δκ pinning centers consisting of the large precipitation, it is thought that the specimens have different sizes of the pinning centers in the samples. So, it can be said that large Y211 particles contribute to flux pinning.

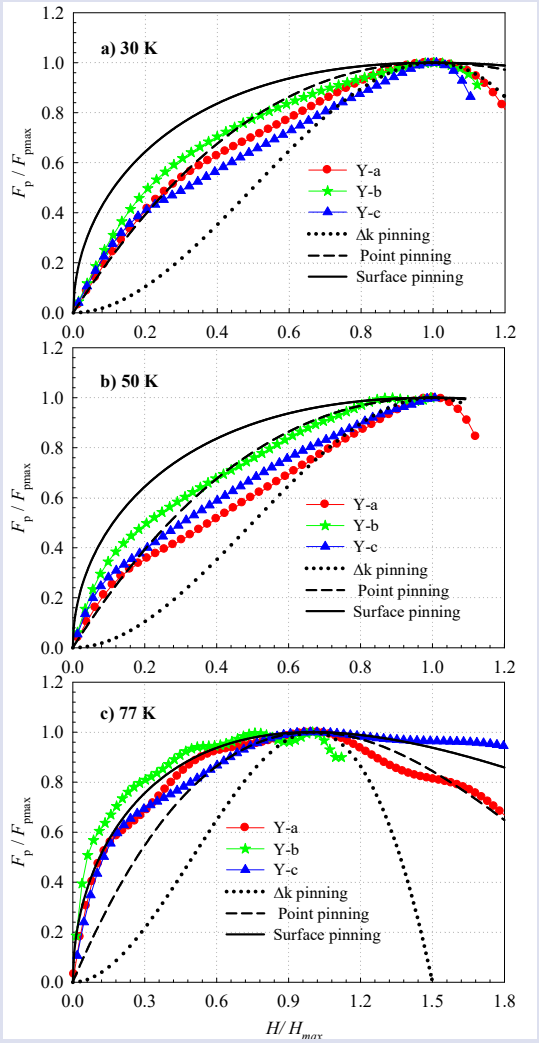

Figure 7. Plots of the normalized pinning force density (f_p) versus reduced field b for the Y-a, Y-b and Y-c samples at a) 30 K, b) 50 K and c) 77 K. Dotted line is the fit curve of Equation (2) for Δκ pinning, dashed line is the fit curve of Equation (3) for normal point-pinning and solid line is the fit curve of Equation (4) for surface pinning.

Conclusions

The pinning force scaling were analyzed for various specimens cut from the different location of the whole TSMG Y123 which is having different number, size and distribution of defects (Y211 inclusions, dislocation, stacking fault etc.). Observed (00ℓ) peaks indicate an orientation in *c*-axis for all the specimens and states that single crystal behavior. The J_c value of the specimen cut from the close region to the seed of the top surface is higher than the specimens taken from the more extreme and lower regions of the sample. This difference in the J_c value change with depending on the number of 211 particles acting as the effective pinning center. The dominant pinning mechanism was normal point pinning (at 30 and 50 K) and surface pinning (at 77 K) below the low field region. The mechanism changed from Δκ to normal point pinning (at 30 and 50 K) and changed from Δκ to surface pinning (at 77 K) in $H_{max} > h > 0.2$ field region. Dominant pinning mechanism changes with increasing the applied field and temperature due to the differences in the pinning centers. Observed transitions between the different pinning mechanisms as the applied field intensity increases originates from the different sizes and shapes of the Y211 particles presented into the structures of the samples. Therefore, the inhomogeneous distribution of different types and shapes of defects into the matrix causes the main superconducting properties such as J_c and flux pinning to vary locally. In this study, the defects that cause the superconducting properties to change are the Y211 particles trapped in the main matrix during the crystal growth process.

Acknowledgment

This work was supported by the Scientific Research Support Fund of The Artvin Çoruh University, Artvin, Turkey, project number 2017.M80.02.02. The author would like to thank Prof. Dr. Alev AYDINER for valuable comments and useful discussions and Dr. Şeyda DUMAN for their help in experimental work.

Conflicts of interest

The author states that did not have conflict of interests

References

[1] Yamachi N., Sakai N., Murakami M., Measurements of three-dimensional fields of bulk superconductors in varying external fields, *Supercond. Sci. Technol.*, 18 (2005) S67-S71.

[2] Ikeda Y., Umakoshi S., Wongsatanawarid A., Seki H., Murakami M., Enhancement of mechanical strength in YBaCuO bulk superconductor through liquid binder addition, *Physica C*, 471 (2011) 846-849.

[3] Lu Y., He D., Liu M., Magnetic force investigation of high-T_c superconducting bulk over permanent magnet railway under different lateral offsets with experimental methods, *J. Mod. Phys.*, 4 (2013) 24-28.

[4] Crisan A., Dang V.S., Mikheenko P, Nano-engineered pinning centres in YBCO superconducting films, *Physica C*, 533 (2017) 118-132.

[5] Slimani Y., Almessiere M.A., Hannachi E., Baykal A., Manikandan A., Mumtaz M., Ben Azzouz F., Influence of WO_3 nanowires on structural, morphological and flux pinning ability of $YBa_2Cu_3O_y$ superconductor, *Ceramics International*, 45(2) (2019) 2621-2628.

[6] Wang Y., Fundamental elements of applied superconductivity in electrical engineering. First. ed. Singapore: Science Press, John Wiley & Sons, (2013).

[7] Ren H.T., Xiao L., Jiao Y.L., Zheng M.H., Processing and characterization of YBCO superconductors by top-seeded melt growth method in batch process, *Physica C*, 412–414 (2004) 597–601.

[8] Hari Babu N., Jackson K.P., Dennis A.R., Shi Y.H., Mancini C., Durrell J.H., Cardwell D.A., Growth of large sized $YBa_2Cu_3O_7$ single crystals using the top seeded melt growth process, Supercond. Sci. Technol., 25 (2012) 075012.

[9] Zhai W., Shi Y., Durrell J.H., Dennis A.R., Cardwell D.A., The influence of Y211 content on the growth rate and Y211 distribution in Y−Ba−Cu−O single grains fabricated by top seeded melt growth, *Cryst. Growth Des.*, 14 (2014) 6367−6375.

[10] Volochova D., Kavecansky V., Antal V., Diko P., Yao X., Thermal stability of NdBCO/YBCO/MgO thin film seeds, *Supercond. Sci. Technol.*, 29 (2016) 044004.

[11] Yang W.M., Yuan X.C., Guo Y.X., Inuence of ZnO doping on the properties of single domain YBCO bulks fabricated by RE+011 TSIG process, *Int. J. Mod. Phys. B.*, 31(25) (2017) 1745018.

[12] Namburi D.K., Shi Y., Dennis A.R., Durrell J.H., Cardwell D.A., A robust seeding technique for the growth of single grain (RE)BCO and (RE)BCO–Ag bulk superconductors, *Supercond. Sci. Technol.*, 31 (2018) 044003.

[13] Xu Y., Izumi M., Tsuzuki K., Zhang Y., Xu C., Murakami M., Sakai N., Hirabayashi I., Flux pinning properties in a $GdBa_2Cu_3O_{7-\delta}$ bulk superconductor with the addition of magnetic alloy particles, *J. Supercond. Nov. Magn.*, 22(9) (2009) 095009.

[14] Aydıner A., Çakır B., Başoğlu M., Seki H., Wongsatanawarid A., Murakami M., Yanmaz E., Magnetic properties of YBCO single-crystal grown on Y2O3 layer by a cold top-seeding method, *J. Supercond. Nov. Magn.*, 25 (2012) 391–397.

[15] Dew-Huges D., Flux pinning mechanism in type II superconductors, *Philisophical Magazine*, 30(2) (1974) 293-305.

[16] Taylan Koparan E., Surdu A., Sidorenko A., Yanmaz E., Artificial pinning centers created by Fe_2O_3 coating on MgB_2 thin films, *Physica C*, 473 (2012) 1-5.

[17] Li M., Chen L., You W-L., Ge J., Zhang J., Giant increase of critical current density and vortex pinning in Mn doped $K_xFe_{2-y}Se_2$ single crystals, *Appl. Phys. Lett.*, 105 (2014) 192602.

[18] Çakır B., Taylan Koparan E., Savaşkan B., Relationship between pinning mechanism and excess conductivity analysis of x wt% $C_4H_6O_5$ (x= 0.0, 4.0 and 6.0) added bulk MgB_2, *J. Mater. Sci.: Mater. Electron.*, 32(15) (2021) 20317-20326.

[19] Duman Ş., Çakır B., Aydıner A., Fluctuation-Induced Conductivity Analysis of Y_2O_3-Layered YBCO Single Crystal, *J. Supercond. Nov. Magn.*, 29 (2016) 2275-2280.

[20] Feng Y., Wen J.G., Pradhan A.K., Koshizuka N., Zhou L., Chen S.K., Wang K.G., Wu X.Z., Preparation and properties of PMP YBCO bulk with submicrometre Y_2BaCuO_5 particles, *Supercond. Sci. Technol.*, 13 (2000) 703-708.

[21] Gupta S., Yadav R.S., Das B., Flux pinning by nano particles embedded in polycrystalline Y-123 superconductors, *arxiv.org*, (2011) 1107/1107.1116.

[22] Crisan A., Dang V.S., Yearwood G., Mikheenko P., Huhtinen H., Paturi P., Investigation of the bulk pinning force in YBCO superconducting films with nano-engineered pinning centres, *Physica C*, 503 (2014) 89-93.

[23] Kim G.C., Kim B.J., Cheon M.Y., Kim Y.C., Variation of pinning mechanism in $Bi_{1.6}Pb_{0.4}Sr_2CaCu_2O_{8+\delta}$ single crystal, *Physica C*, 391 (2013) 305–308.